OPEN ACCESS

University of BRISTOL

Peer reviewed version

Link to published version (if available):
10.1002/anie.201909228

Link to publication record in Explore Bristol Research
PDF-document

University of Bristol - Explore Bristol Research
General rights

Photo-switchable phase separation and oligonucleotide trafficking in DNA coacervate micro-droplets

Nicolas Martin,*[a][b] Liangfei Tian[b][c], Dan Spencer[b], Angélique Coutable-Pennarun[c][d], J. L. Ross Anderson[c][d] and Stephen Mann*[b][c]

[a]   Univ. Bordeaux, CNRS, Centre de Recherche Paul Pascal, UMR5031, 115 Avenue du Dr. Albert Schweitzer, F-33600 Pessac, France
[b]   Centre for Protolife Research and Centre for Organized Matter Chemistry, School of Chemistry, University of Bristol, Bristol, BS8 1TS, UK.
[c]   BrisSynBio Synthetic Biology Research Centre, Life Sciences Building, University of Bristol, Tyndall Avenue, Bristol, BS8 1TQ, UK.
[d]   School of Biochemistry, University of Bristol, University Walk, Bristol, BS8 1TD, UK.

E-mail: nicolas.martin@crpp.cnrs.fr; s.mann@bristol.ac.uk

Abstract: Coacervate micro-droplets produced by liquid-liquid phase separation have been used as synthetic protocells that mimic the dynamical organization of membrane-free organelles in living systems. Achieving spatiotemporal control over droplet condensation and disassembly remains challenging. Herein, we describe the formation and photo-switchable behaviour of light-responsive coacervate droplets prepared from mixtures of double-stranded DNA and an azobenzene cation. The droplets disassemble and reassemble under UV and blue light, respectively, due to azobenzene *trans/cis* photo-isomerisation. Sequestration and release of captured oligonucleotides follows the dynamics of phase separation such that light-activated transfer, mixing, hybridization and trafficking of the oligonucleotides can be controlled in binary populations of the droplets. Our results open perspectives for the spatiotemporal control of DNA coacervates and provide a step towards the dynamic regulation of synthetic protocells.

The dynamic compartmentalization of biological components in space and time is a hallmark of functional synchronization in living cells. Biomolecular condensates formed via liquid-liquid phase separation are dynamic subcellular compartments that are actively formed and dissolved in response to environmental cues.[1,2] They play a crucial role for example in the compaction of polynucleotides and regulation of genetic expression.[3,4] Micro-droplets produced *in vitro* by associative (coacervates) or segregative (aqueous two-phase systems) liquid-liquid phase separation have recently been used as synthetic models of dynamic protocells.[5-7] These membrane-free molecularly crowded compartments sequester functional biomolecules[5,8] and support enzymatic activity,[9,10] protein folding,[11] RNA catalysis[12,13] and cell-free protein expression.[14] Polynucleotides have been used as scaffold components to assemble coacervate droplets,[15-19] and selective sequestration of guest polynucleotides has been demonstrated in preformed coacervates.[12,20,21] Owing to their liquid-like nature and the weak molecular interactions, synthetic coacervate droplets can dynamically respond to external stimuli.[7,22,23] For instance, their formation and dissolution has been achieved by changes in pH,[5] temperature,[24-26] ionic strength,[27,28] and more recently by enzyme-mediated catalytic activity.[15,29-32] However, platforms enabling the rapid and localized actuation of polynucleotide microphase separation have not yet been developed. Due to its favourable spectral and spatiotemporal capabilities, light holds great promise as a programmable trigger for controlling the reversible assembly and disassembly of coacervate droplets. Light has been used to control synthetic micro-compartments,[33-35] trigger biomolecular condensation *in cellulo* via optogenetic tools,[36,37] promote the dynamical shaping of soft colloids[38] and induce the reversible compaction of single DNA chains.[39-41]

Here, we exploit the attractive electrostatic interactions between double stranded DNA (*ds*DNA) and a light-responsive azobenzene cation (*trans*-azobenzenetrimethylammonium bromide; *trans*-azoTAB) to produce liquid-like coacervate micro-droplets that can be disassembled and reassembled within a few seconds with UV and blue light, respectively (**Figure 1a**). The photo-switchable phase separation arises from photo-isomerisation between *trans*-azoTAB and the metastable *cis*-azoTAB isomer. We show that temporal programming of DNA droplet condensation can also be achieved by regulating the spontaneous thermal relaxation of *cis*-azoTAB to *trans*-azoTAB in the dark at varying temperatures. We further demonstrate the light-activated transfer of captured oligonucleotides between physically separated populations of droplets as well as trafficking between spatially interacting binary mixtures of different droplets as a step towards increasing the networking capacity of a consortium of interactive protocells. Given the possibility of transferring genetic polymers between different populations of coacervate droplets, we apply a focused UV beam to induce the localized trafficking of DNA between

single neighbouring droplets. Taken together, our results highlight new approaches for the photo-induced control of DNA coacervation and oligonucleotide compartmentalization in space and time, and provide a step towards the dynamic regulation of membrane-free synthetic protocells.

Light-responsive coacervate micro-droplets were produced in water in the dark as a turbid suspension via spontaneous liquid-liquid phase separation associated with the stoichiometric charge neutralization of short *ds*DNA strands (5 mM nucleobase concentration, <200 base pairs (bp), **Figure S1**) in the presence of *trans*-azoTAB (5 mM) and sodium chloride (100 mM). Optical microscopy images of the suspension revealed the presence of discrete polydisperse spherical droplets approximately 1 to 10 μm in diameter (**Figure 1b**) that coalesced on contact, consistent with a liquid-like state (**Figure S2** and **SI Note 1**), and that were able to selectively sequester various solutes (**Figure S3**). The driving forces responsible for droplet assembly included a combination of electrostatic and hydrophobic interactions, together with partial intercalation of the molecular photoswitch between the *ds*DNA base pairs[39-41] (**Figure S4**).

Although the *trans*-azoTAB/*ds*DNA micro-droplets were stable across a wide range of ionic strengths, pHs and temperatures (**Figures S4** and **S5**), they readily disassembled within a few seconds when exposed to UV light (λ = 365 nm, **Figure 1c**, **Movie S1** and **Figure S6**). We attributed the light-activated droplet disassembly to the reversible photo-isomerisation of *trans*-azoTAB into the non-planar *cis*-azoTAB metastable isomer, which exhibits a lower affinity for *ds*DNA[39-41] (**Figure S4** and **S7**). Coacervate droplets could be re-assembled by irradiating solutions of *cis*-azoTAB/*ds*DNA with blue light (λ = 450 nm), which re-generated the thermodynamically stable *trans*-azoTAB isomer (**Figure 1d**, **Movie S2** and **Figure S6**). Significantly, the kinetics of the photo-switchable phase separation could be finely modulated by adjusting the light intensity, and the process repeated over numerous cycles without any apparent degradation (**Figure S8**).

The dynamics of droplet disassembly and re-assembly were exploited for the correlated release and recapture of sequestered guest molecules. For example, doping dark-adapted *trans*-azoTAB/*ds*DNA droplets with a fluorescent single-stranded oligonucleotide (TAMRA-*ss*DNA, 23 nucleobases) and exposing the loaded droplets to UV light showed a gradual and quantitative release of the oligonucleotide into the surrounding aqueous phase (**Figures 1e,f**). Subsequent exposure of the *cis*-azoTAB/*ds*DNA solution to blue light re-assembled the droplets and recaptured approximately 80% of the oligonucleotide (**Figures 1e,f**). Alternatively, temporal programming of DNA phase separation was achieved by controlling the spontaneous thermal relaxation of *cis*- to *trans*-azoTAB in the dark. Optical microscopy images of a UV-equilibrated *cis*-azoTAB/*ds*DNA solution incubated in the dark confirmed a gradual increase in the number and size of coacervate droplets (**Figure 1g**). The corresponding changes in turbidity showed a sigmoidal increase, consistent with a kinetically slow nucleation step followed by rapid growth up to the saturation limit (**Figure 1h**). Significantly, the onset time for phase separation was strongly correlated with the temperature following a simple Arrhenius law (**Figure S9** and **Table S2**), demonstrating that DNA phase separation could be robustly programmed in time. For example, by exposing *trans*-azoTAB/*ds*DNA droplets to cycles comprising short periods of UV light irradiation followed by storage in the dark at a specific temperature, predictable oscillations in the time-dependent concentration of free TAMRA-*ss*DNA could be realized (**Figure S10**).

Given the above observations, we sought to increase the networking capacity of the photoactive coacervate system by undertaking experiments geared towards controlling the photo-induced trafficking of captured oligonucleotides. We devised an experimental system in which oligonucleotide-containing photo-responsive coacervate droplets and payload-free non-photo-responsive droplets were physically separated by a semi-permeable barrier and then used UV light to induce transfer of the oligonucleotide between the two populations (**Figure 2a**). Specifically, *trans*-azoTAB/*ds*DNA droplets containing TAMRA-ssDNA and non-photo-responsive poly(diallyldimethylammonium chloride) (PDDA)/*ds*DNA droplets were loaded in the dark into two separate sample chambers arranged on a capillary slide and separated by an agarose hydrogel barrier. Corresponding optical and fluorescence microscopy images showed the presence of discrete droplets in both populations but only the *trans*-azoTAB/*ds*DNA droplets displayed red fluorescence due to retention of TAMRA-*ss*DNA (**Figures 2b,c**). In contrast, when the capillary slide was irradiated with UV light, dissolution of the light-responsive droplets resulted in the release of the oligonucleotide, slow diffusive transfer across the hydrogel barrier and graded capture of the payload in the population of PDDA/*ds*DNA droplets (**Figure 2d** and **Figure S11**).

We employed a related strategy to control the light-activated transfer and manipulation of genetic information within dispersed binary populations of spatially interacting photo-responsive coacervate micro-droplets. Populations of *trans*-azoTAB/*ds*DNA coacervate droplets containing fluorescence resonance energy transfer (FRET)-paired complementary single strands of TAMRA-*ss*DNA or carboxyfluorescein-labelled *ss*DNA (FAM-*ss*DNA, 23 nucleobases) were mixed in the same observation chamber and sequentially exposed to UV and blue light (**Figure 3a** and **Table S3**). Confocal

fluorescence microscopy revealed the co-existence of two distinct droplet populations that exhibited either red fluorescent (TAMRA-*ss*DNA payload) or green fluorescent (FAM-*ss*DNA payload) (**Figure 3b**). No spontaneous *ss*DNA exchange between the droplets was observed for samples kept in the dark. In comparison, disassembly of the droplets under UV light followed by reassembly after exposure to blue light produced droplets that exhibited both green and red fluorescence (**Figure 3c**), indicating that the complementary strands became co-localized via reversible photo-induced microphase separation. Moreover, the co-localized strands displayed increased FRET fluorescence, which was attributed to hybridization of the released oligonucleotides either prior to droplet re-assembly or within the droplets after colocalization, or both (**Figure 3d**).

Given the ability to transfer genetic polymers between different populations of coacervate droplets, we used a focused UV beam to induce the localized trafficking of DNA between single neighbouring droplets (**Figure 3e**). For this purpose, a mixture of unloaded and TAMRA-*ss*DNA-loaded *trans*-azoTAB/*ds*DNA coacervate droplets was prepared and imaged by confocal fluorescent microscopy combined with bright-field microscopy, which confirmed the co-existence of two types of coacervate droplets that appeared either dark (non-fluorescent) or exhibited red fluorescence (**Figure 3f**, $t = t_0$). No exchange of the payload was observed in the dark. A brief UV light pulse (1 s) was then focused on a single TAMRA-*ss*DNA-containing droplet that was located close to a non-fluorescent counterpart. We were able to disassemble the target droplet without affecting the neighbouring droplets such that TAMRA-*ss*DNA was ejected locally into the supernatant and subsequently captured by the adjacent non-fluorescent droplet, which showed a gradual increase in red fluorescence over a period of approximately 100s (**Figures 3f-h** and **Movie S3**). From the fluorescence intensity measurements, we estimated that approximately 20% of the released *ss*DNA was typically captured by the neighbouring droplet depending on the diffusion distance. The locally induced chemical gradient of free TAMRA-*ss*DNA established immediately after UV-induced disassembly of the single droplet gave rise to an initially asymmetric distribution of the captured oligonucleotide droplet that became homogeneous with time (**Figure 3f**, $t = t_0 + 1.4s$, and **Figure 3g**). A similar light-mediated pathway for the diffusion-limited trafficking of *ss*DNA was demonstrated between multiple co-located coacervate micro-droplets by sequential UV processing of individual TAMRA-*ss*DNA-containing droplets and neighbouring unloaded droplets (**Figure S12**).

In conclusion, we describe a new light-responsive DNA coacervate with photo-switchable behaviour that exhibits controllable droplet dynamics and light-activated trafficking of guest molecules. Our results highlight opportunities for controlling the spatiotemporal dynamics of DNA-containing protocells and their interplay in communities of artificial cells. For example, as DNA has been used to achieve cell-free protein expression in coacervate droplets[14] and develop programmable logic gates in synthetic protocells,[42] light-actuated DNA coacervation could be exploited to activate signalling pathways in populations of active droplets or synthetic protocells, paving the way to the construction of life-like colloidal systems capable of spatiotemporally coordinated behaviours.

Conflict of interest
The authors declare no conflict of interest.

References
[1]   C. P. Brangwynne, C. R. Eckmann, D. S. Courson, A. Rybarska, C. Hoege, J. Gharakhani, F. Jülicher, A. A. Hyman, *Science*, **2009**, *324*, 1729-1732.
[2]   R. J. Wheeler, A. A. Hyman, *Phil. Trans. R. Soc. B* **2017**, *373*, 20170193.
[3]   S. C.Weber, C. P. Brangwynne, *Cell* **2012**, *149*, 1188-1191.
[4]   S. Maharana *et al. Science* **2018**, *360*, 918-921.
[5]   S. Koga, D. S. Williams, A. W. Perriman, S. Mann, *Nat. Chem.* **2011**, *3*, 720-724.
[6]   M. S. Long, C. D. Jones, M. R. Helfrich, L. K., Mangeney-Slavin, C. D. Keating, *Proc. Natl. Acad. Sci.* **2005**, *102*, 5920-5925.
[7]   N. Martin, *ChemBioChem* **2019**, *in press*, doi:10.1002/cbic.201900183
[8]   P. M. McCall, S. Srivastava, S. L. Perry, D. R. Kovar, M. L. Gardel, M. V. Tirrell, *Biophys. J.* **2018**, *114*, 1636-1645.
[9]   B. W. Davis, W. M. Aumiller, N. Hashemian, S. An, A. Armaou, C. D. Keating, *Biophys. J.* **2015**, *109*, 2182-2194.

[10] J. Crosby, T. Treadwell, M. Hammerton, K. Vasilakis, M. P. Crump, D. S. Williams, S. Mann, *Chem. Commun.* **2012**, *48*, 11832-11834.

[11] N. Martin, M. Li, S. Mann, *Langmuir* **2016**, *32*, 5881-5889.

[12] B. Drobot, J. M. Iglesias-Artola, K. Le Vay, V. Mayr, M. Kar, M. Kreysing, H. Mutschler, T. Y. D. Tang, *Nat. Commun.* **2018**, *9*, 3643.

[13] R. R. Poudyal, R. M. Guth-Metzler, A. J. Veenis, E. A. Frankel, C. D. Keating, P. C. Bevilacqua, *Nat. Commun.* **2019**, *10*, 490.

[14] T. Y. D. Tang, D. van Swaay, A. deMello, J. L. R. Anderson, S. Mann, *Chem. Commun.* **2015**, *51*, 11429-11432.

[15] W. M. Aumiller Jr, C. D. Keating, *Nat. Chem.* **2016**, *8*, 129-137.

[16] J. R. Vieregg, T. Y. D. Tang, *Curr. Opin. Colloid. Int. Sci.* **2016**, *26*, 50-571.

[17] P. R. Banerjee, A. N. Milin, M. M. Moosa, P. L. Onuchic, A. A. Deniz, *Angew. Chem. Int. Ed.* **2017**, *56*, 11354-11359.

[18] J. R. Vieregg, M. Lueckheide, A. B. Marciel, L. Leon, A. J. Bologna, J. Reyes Rivera, M. V. Tirrell *J. Am. Chem. Soc.* **2018**, *140*, 1632-1638.

[19] A. Shakya, J. T. King, *Biophys. J.* **2018**, *115*, 1840-1847.

[20] Y. Qiao, R. Booth, M. Li, S. Mann, *Nat. Chem.* **2017**, *9*, 110-119.

[21] T. J. Nott, T. D. Craggs, A. J. Baldwin, *Nat. Chem.* **2016**, *8*, 569-575.

[22] N. Martin, J. P. Douliez, Y. Qiao, R. Booth, M. Li, S. Mann, *Nat. Commun.* **2018**, *9*, 3652.

[23] J. P. Douliez, N. Martin, C. Gaillard, T. Beneyton, J. C. Baret, S. Mann, L. Béven, *Angew. Chem. Int. Ed.* **2017**, *56*, 13689-13693.

[24] N.N. Deng, W. T. S. Huck, *Angew. Chem. Int. Ed.* **2017**, *56*, 9736-9740.

[25] J. R. Simon, N. J. Carroll, M. Rubinstein, A. Chilkoti, G. P. Lopez, *Nat. Chem.* **2017**, *6*, 509-515.

[26] R. Mérindol, S. Loescher, A. Samanta, A. Walther, *Nat. Nanotech.* **2018**, *13*, 730-738.

[27] S. L. Perry, Y. Li, D. Priftis, L. Leon, M. Tirrell, *Polymers* **2014**, *6*, 1756-1772.

[28] Q. Wang, J.B. Schlenoff, *Macromolecules* **2014**, *47*, 3108-3116.

[29] K. K. Nakashima, J. F. Baaji, E. Spruijt, *Soft Matter* **2018**, *14*, 361-367.

[30] B. S. Schuster, E. H. Reed, R. Parthasarathy, C. N. Jahnke, R. M. Caldwell, J. G. Bermudez, H. Ramage, M. C. Good, D. A. Hammer, *Nat. Commun.* **2018**, *9*, 2985.

[31] S. S. Yang, B. Li, C. Wu, W. Xu, M. Tu, Y. Yan, J. Huang, M. Dreschler, S. Granick, L. Jiang, *ACS Nano,* **2019**, *13*, 2420-2426.

[32] S. Deshpande, F. Brandenburg, A. Lau, M. G. F. Last, W. K. Spoelstra, L. Reese, S. Wunnava, M. Dogterom, C. Dekker *Nat. Commun.* **2019**, *10*, 1800.

[33] A. Diguet, M. Yanagisawa, Y.-J. Liu, E. Brun, S. Abadie, S. Rudiuk, D. Baigl, A. *J. Am. Chem. Soc.* **2012**, *134*, 4898-4904.

[34] A. Peyret, E. Ibarboure, A. Tron, L. Beauté, R. Rust, O. Sandre, N. D. McClenaghan, D. Lecommandoux*, Angew. Chem. Int. Ed.* **2017**, *56*, 1566-1570.

[35] S. M. Bartelt, J. Steinkuhler, R. Dimova, S. V. Wegner, *Nano Lett.* **2018**, *18*, 7268-7274.

[36] Y. Shin, J. Berry, N. Pannucci, M. P. Haataja, J. E. Toettcher, C. P. Brangwynne, *Cell.* **2017**, *168*, 159-171.

[37] D. Bracha, M. T. Walls, M.-T. Wei, L. Zhu, M. Kurian, J. L. Avalos, J. E. Toettcher, C. P. Brangwynne, *Cell.* **2018**, *175*, 1467-1480.

[38] N. Martin, K. P. Sharma, R. L. Harniman, R. M. Richardson, R. J. Hutchings, D. Alibhai, M. Li, S. Mann*, Sci. Rep.* **2017**, *7*, 41327.

[39] A. L. M. Le Ny, C. T. Lee Jr, *J. Am. Chem. Soc.* **2006**, *128*, 6400-6408.

[40] a) M. Sollogoub, S. Guieu, M. Geoffroy, A. Yamada, A. Estevez-Torres, K. Yoshikawa, D. Baigl, *ChemBioChem*, **2008**, *9*, 1201-1203, b) A. Diguet, N. K. Mani, M. Geoffroy, M. Sollogoub, D. Baigl, D. *Chem. Eur. J.* **2010**, *16*, 11890-11896, c) A. Estevez-Torres, C. Crozatier, A. Diguet, T. Hara, H. Saito, K. Yoshikawa, D. Baigl, *Proc. Natl. Acad. Sci.* **2009**, *106*, 12219-12223, d) A. Venancio-Marques, A. Bergen, C. Rossi-Gendron, S. Rudiuk, D. Baigl *ACS Nano*, **2014**, *8*, 3654-3663.

[41] Y. Zakrevskyy, A. Kopyshev, N. Lomadze, E. Morozova, L. Lysyakova, N. Kasyanenko, S. Santer, *Phys. Rev. E* **2011**, *84*, 021909.

[42] A. Joesaar*,* S. Yang, B. Bogels, A. van der Linden, P. Pieters, B. V. V. S. Pavan Kumar, N. Dalchau, A. Philips, S. Mann, T. F. A. de Greef *Nat. Nanotechnol.* **2019***, 14*, 369–378.
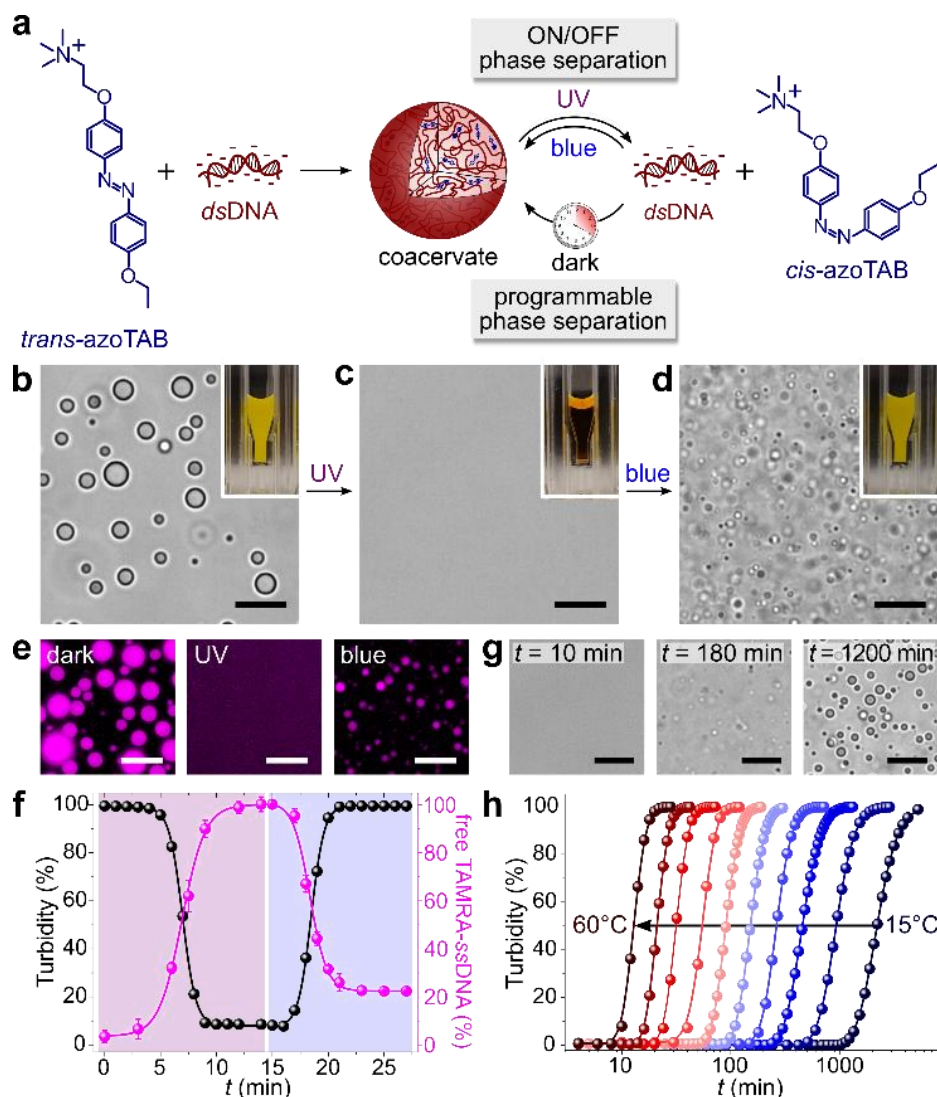
Figure 1. a) Scheme of the associative liquid-liquid phase separation of *trans*-azoTAB and *ds*DNA to produce coacervate droplets that are disassembled under UV light by isomerisation to *cis*-azoTAB and reassembled under blue light (on/off process). Programming of the reassembly process is achieved by regulating the *cis-trans* thermal relaxation in the dark at varying temperatures. b-d) Optical microscopy images of azoTAB (5 mM) mixed with *ds*DNA (5 mM nucleobase concentration) in the presence of 100 mM NaCl at pH 8 in the dark (b), under UV light (c), and under blue light after UV light exposure (d); scale bars, 10 μm. Insets show photographs of the corresponding turbid suspensions (dark or blue light), or the clear solution (UV). e) Fluorescence microscopy images of *trans*-azoTAB/*ds*DNA coacervates in the dark doped with TAMRA-*ss*DNA (left), and after sequential exposure to UV (centre) and then blue (right) light, showing release and re-sequestration of the oligonucleotide (false colouring to magenta). Scale bars, 10 μm. f) Plots of turbidity (black circles) and fraction of TAMRA-*ss*DNA free in solution (magenta circles) against time for TAMRA-*ss*DNA-doped *trans*-azoTAB/*ds*DNA droplets after sequential exposure to UV (purple area) and then blue (blue area) light. Error bars represent standard deviations of the average value measured on three different samples. g) Time series of optical microscopy images of a UV-adapted *cis*-azoTAB/*ds*DNA solution stored at 35°C in the dark, showing gradual nucleation and growth of *trans*-azoTAB/*ds*DNA droplets via spontaneous *cis-trans* thermal relaxation; scale bars, 10 μm. h) Plots showing time-dependent increase of the turbidity of UV-equilibrated *cis*-azoTAB/*ds*DNA solutions stored in the dark at varying temperatures (from 15°C (right, dark blue circles) to 60°C (left, dark red circles) in 5°C intervals).
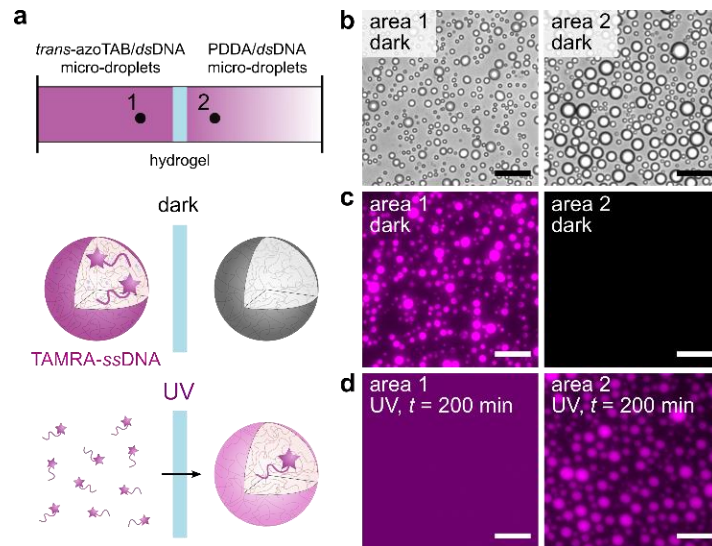
Figure 2. a) Scheme of light-activated oligonucleotide transfer from *trans*-azoTAB/*ds*DNA droplets (area **1**) to photo-inactive PDDA/*ds*DNA droplets (area **2**) across an agarose hydrogel barrier. TAMRA-*ss*DNA is retained within the light-responsive droplets in the dark but released on exposure to UV. Diffusive transfer of the oligonucleotides through the hydrogel gives rise to sequestration of the payload in the PDDA/*ds*DNA droplets. b-d) Brightfield (b) and epifluorescence (c,d) microscopy images of areas **1** and **2** in the dark (b,c) and after 210 min of UV light irradiation (d), showing transfer of TAMRA-*ss*DNA to the PDDA/*ds*DNA droplets (false colouring to magenta used). The mean grey values were adjusted between 0 and 45 on the fluorescence images of area **2** to emphasize low levels of fluorescence, while they were left between 0 and 255 on the fluorescence images of area **1**. Scale bars, 20 µm.
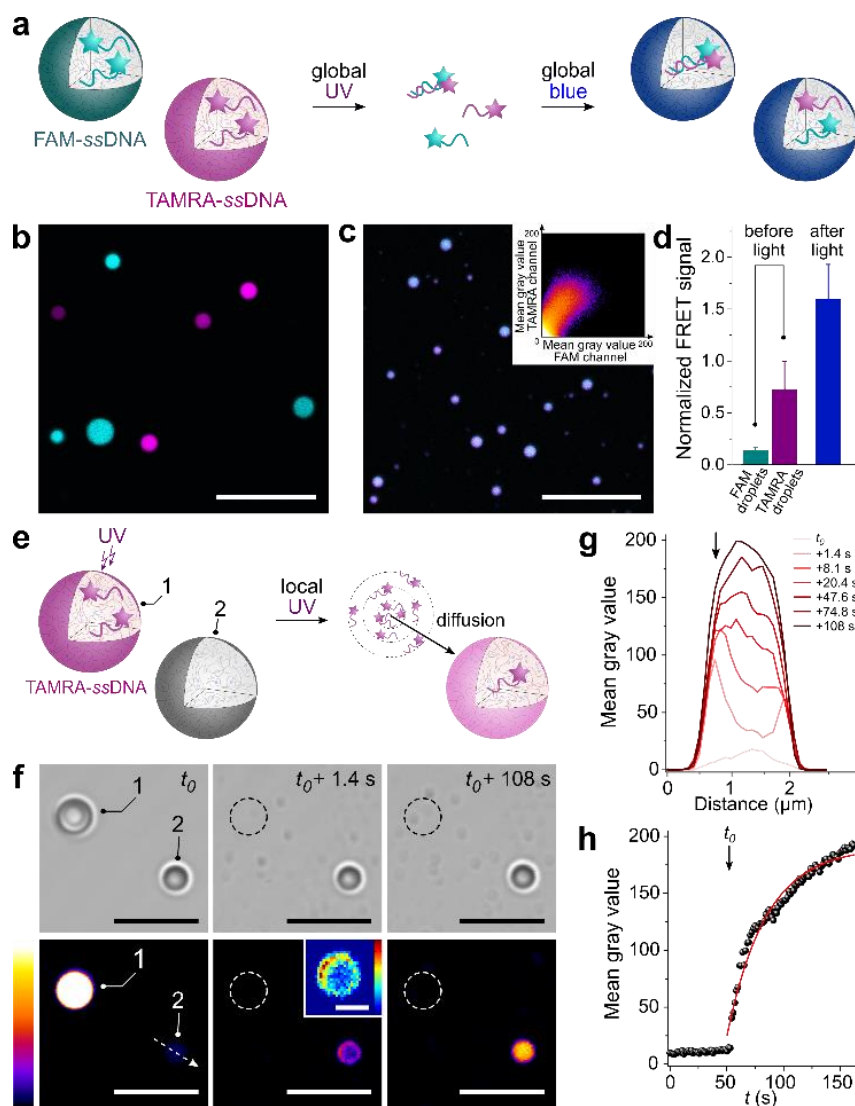
Figure 3. a) Scheme of light-activated oligonucleotide mixing and hybridization in a binary population of *trans*-azoTAB/*ds*DNA coacervate droplets containing complementary TAMRA-*ss*DNA or FAM-*ss*DNA. UV-induced release of the oligonucleotides results in FRET pairing. Subsequent exposure to blue light results in reassembly of the droplets and capture of the hybridized strands. b,c) Confocal fluorescence microscopy images of a binary population of *trans*-azoTAB/*ds*DNA droplets doped with TAMRA-*ss*DNA or FAM-*ss*DNA (false colouring to magenta and cyan, respectively), before (b) and after (c) sequential exposure to UV and blue light. Inset in c shows co-localization scatterplot (Pearson's correlation constant, ρ = 0.79)). Scale bars, 20 μm. d) Normalized FRET signal in droplets before and after sequential UV-then-blue light irradiation, showing low level of FRET signal in droplets containing only FAM-*ss*DNA or TAMRA-*ss*DNA (before light), and increased FRET signal in droplets containing both oligonucleotides (after light). Error bars represent standard deviation from the average value measured on 20 droplets in three different fields of view of the same sample. e) Scheme of UV light-activated trafficking of oligonucleotides from a single photo-switchable *trans*-azoTAB/*ds*DNA droplet doped with TAMRA-*ss*DNA (droplet **1**) to a second non-fluorescent *trans*-azoTAB/*ds*DNA droplet devoid of oligonucleotide (droplet **2**). A short (1 s) UV pulse focused on **1** results in release of the payload followed by its diffusion and sequestration within **2**. f) Optical (top) and confocal fluorescence (bottom) microscopy images of two different droplets (**1** and **2**) before and after droplet **1** is exposed briefly to UV light (at $t = t_0$). Selective disassembly of **1** is observed at $t = t_0 + 1.4$ s along with the early stages of TAMRA-*ss*DNA transfer to **2**. Inset at $t = t_0 + 1.4$ s displays an enlarged image of droplet **2** in false colouring (colour scale from 10 to 140) showing the initial localized increase in fluorescence intensity on the side of the droplet closest to the diffusion front emanating from droplet **1**. False colouring is used to emphasize low levels of fluorescence (colour scale from 0 to 255 mean grey value). Scale bars, 10 μm and 1 μm (inset). g) Time-dependent evolution of line profiles across droplet **2** (white dotted arrow at $t = t_0$ in f); black arrow denotes edge of droplet **2** closest to the disassembling droplet **1**. h) Plot of the mean fluorescence intensity at the centre of droplet **2** as a function of time before and after targeted disassembly of droplet **1** (at $t = t_0$). The red line is a fit to a mono-exponential function.